# Time-resolved observation of thermalization in an isolated quantum system

Article (Published Version)

# Time-Resolved Observation of Thermalization in an Isolated Quantum System

Govinda Clos,[1,*] Diego Porras,[2] Ulrich Warring,[1] and Tobias Schaetz[1]
[1]Physikalisches Institut, Albert-Ludwigs-Universität, Hermann-Herder-Straße 3, 79104 Freiburg, Germany
[2]Department of Physics and Astronomy, University of Sussex, Brighton BN1 9QH, United Kingdom
(Received 13 May 2016; revised manuscript received 5 August 2016; published 19 October 2016)

We use trapped atomic ions forming a hybrid Coulomb crystal and exploit its phonons to study an isolated quantum system composed of a single spin coupled to an engineered bosonic environment. We increase the complexity of the system by adding ions and controlling coherent couplings and, thereby, we observe the emergence of thermalization: Time averages of spin observables approach microcanonical averages while related fluctuations decay. Our platform features precise control of system size, coupling strength, and isolation from the external world to explore the dynamics of equilibration and thermalization.

DOI: 10.1103/PhysRevLett.117.170401

How does statistical mechanics emerge from the microscopic laws of nature? Consider, for example, a finite, isolated quantum system: It features a discrete spectrum and a quantized phase space, its dynamics are governed by the linear Schrödinger equation and, thus, remain reversible at all times. Can such a system equilibrate or even thermalize? Progress in the theory of nonequilibrium dynamics and statistical mechanics sheds light on these fundamental questions. It has been shown that individual quantum states can exhibit properties of thermodynamics depending on entanglement within the system [1–7]. While the entire system may very well be described by a pure state, any small subsystem and related local observables may be found in a mixed state due to disregarded entanglement with the rest of the isolated system, i.e., the large environment. Further, it is predicted that even any individual many-body eigenstate of a nonintegrable Hamiltonian yields expectation values for few-body observables that are indistinguishable from microcanonical averages [8–13]. This conjecture has been extensively studied by numerical simulations of specific quantum many-body systems of moderate size, exploiting available computational power [14–17]. Recently, there have been first experiments in the context of thermalization in closed quantum systems with ultracold atoms [18–20]. However, fundamental questions on the underlying microscopic dynamics of thermalization and its time scales remain unsettled [12,21,22].

Trapped-ion systems are well suited to study quantum dynamics at a fundamental level, featuring unique control in preparation, manipulation, and detection of electronic and motional degrees of freedom [23–29]. Their Coulomb interaction of long range permits tuning from weak to strong coupling [30]. Additionally, systems can be scaled bottom up to the mesoscopic size of interest to investigate many-body physics [31–34].

In this Letter, we study linear chains of up to five trapped ions using two different isotopes of magnesium to realize a single spin with tunable coupling to a resizable bosonic environment. Time averages of spin observables become indistinguishable from microcanonical ensemble averages, and amplitudes of time fluctuations decay as the effective system size is increased. We observe the emergence of statistical mechanics in a near-perfectly-isolated quantum system, despite its seemingly small size.

The dynamics of our system are governed by the Hamiltonian [35,36]

$$H=\frac{\hbar\omega_z}{2}\sigma_z+\frac{\hbar\Omega}{2}\sigma_x+\sum_{j=1}^{N}\hbar\omega_j a_j^\dagger a_j+\frac{\hbar\Omega}{2}(\sigma^+C+\sigma^-C^\dagger). \quad (1)$$

The spin is described by Pauli operators $\sigma_l (l = x, y, z)$ and $\hbar$ denotes the reduced Planck constant. The first term can be interpreted as interaction of the spin with an effective magnetic field $\omega_z$, lifting degeneracy of the eigenstates of $\sigma_z$, labeled $|\downarrow\rangle$ and $|\uparrow\rangle$, while the second drives oscillations between these states with spin coupling rate $\Omega$. The sum represents the environment composed of $N$ harmonic oscillators with incommensurate frequencies $\omega_j$, and the operators $a_j$ $(a_j^\dagger)$ annihilate (create) excitations, i.e., phonons, of mode $j$. The last term describes spin-phonon coupling via spin flips, $\sigma^\pm \equiv (\sigma_x \pm i\sigma_y)/2$, accompanied by motional (de)excitation, which is incorporated in

$$C = \exp\left[i\sum_{j=1}^{N}\eta_j(a_j^\dagger + a_j)\right] - 1, \quad (2)$$

at a strength tunable by $\Omega$ and the spin-phonon coupling parameters $\eta_j \propto 1/\sqrt{\omega_j}$. Expanding $C$ in series permits restricting to linear terms for values $\eta_j \ll 1$ (weak coupling). For $\eta_j \approx 1$, as in our experiment, higher order terms become significant (strong coupling), allowing the system to explore the full many-body set of highly entangled spin-phonon states. This regime is well described by full exact diagonalization (ED) only, since the discrete nature of the bosonic environment of finite size hinders standard approximations applicable to the spin-boson model considering a continuous spectral density [36,47].

To study nonequilibrium dynamics of expectation values $\langle\sigma_l(t)\rangle (l = x, y, z)$, consider an initial product state

 

$\rho(t=0) \equiv \rho(0) = \rho_S(0) \otimes \rho_E(0)$, where the spin is in a pure excited state and the bosonic modes are cooled close to their motional ground states (average occupation $\bar{n}_{j=1,\ldots,N} \lesssim 1$). With this, we ensure that energies of spin and phonons remain comparable to enable the observation of the coherent quantum nature of the dynamics which creates entanglement of spin and phonon degrees of freedom. Because of the coupling, the spin subsystem is in a mixed state for $t > 0$, even though the entire system is evolving unitarily. When thermalization occurs, any small subsystem of a large isolated system equilibrates towards a thermal state and remains close to it for most times [4,10].

The so-called eigenstate thermalization hypothesis provides a potential explanation for the emergence of thermalization in an isolated quantum system. It can be phrased as a statement about matrix elements of few-body observables in the eigenstate basis of a many-body Hamiltonian [8–13]. Within this conjecture, infinite-time averages of expectation values of these observables agree with microcanonical averages. A mathematical definition of this hypothesis and further information are given in the Supplemental Material [36]. Based on Refs. [8,9], to interpret experimental results, we assume that a coupling distributes any of the energy eigenstates of an uncoupled system $\{|\phi_\alpha\rangle\}$ over a large subset of the energy eigenstates of the coupled system $\{|\psi_\beta\rangle\}$; i.e., $|\phi_\alpha\rangle = \sum_\beta c_\beta(\alpha)|\psi_\beta\rangle$ [36]. Further, we consider that these participating states lie within a narrow energy shell around the energy of $|\phi_\alpha\rangle$ [11,13]. As introduced in Refs. [1,4,6,10], an effective dimension of the subset, $d_{\text{eff}} \equiv 1/\text{tr}(\rho^2)$, provides an estimation for the ergodicity of a system. It has been shown that mean amplitudes of time fluctuations of expectation values are bounded by $1/\sqrt{d_{\text{eff}}}$ [4,6].

Correspondingly, for our system, we exploit these predictions for infinite-time averages, both of spin expectation values,

$$\mu_\infty(\langle\sigma_l\rangle) \equiv \lim_{\tau\to\infty} \frac{1}{\tau} \int_0^\tau dt \langle\sigma_l(t)\rangle, \tag{3}$$

and of their time fluctuations,

$$\delta_\infty(\langle\sigma_l\rangle) \equiv \sqrt{\mu_\infty(\langle\sigma_l\rangle^2) - \mu_\infty(\langle\sigma_l\rangle)^2}. \tag{4}$$

To this end, we need to quantify the complexity of the dynamics induced by the coupling. Hence, we extend existing definitions of $d_{\text{eff}}$ to a weighted effective dimension [36],

$$D_{\text{eff}} \equiv \sum_\alpha w_\alpha \left( \sum_\beta |c_\beta(\alpha)|^4 \right)^{-1}, \tag{5}$$

for $\rho(0) = \sum_\alpha w_\alpha |\phi_\alpha\rangle\langle\phi_\alpha|$. Here, in contrast to $d_{\text{eff}}$, the statistical average over $w_\alpha$ is performed after calculating the inverse participation ratio for each pure state in the mixture [36]. Thereby, $D_{\text{eff}}$ also incorporates the number of participating states, but is normalized to $D_{\text{eff}} = 1$ for the uncoupled system.

Throughout our Letter, we estimate $D_{\text{eff}}$ numerically. $D_{\text{eff}}$ depends on $N$, $\Omega$, $\omega_z$, $\eta_1$, and $\rho(0)$. We approximate the latter by truncating the Hilbert space $\mathcal{H}$ to $\mathcal{H}_{\text{trunc}}$, choosing a phonon number cutoff $n_c$, such that $\dim(\mathcal{H}_{\text{trunc}}) = 2(n_c+1)^N \lesssim 2^{16}$ [36]. For a given computational power and increasing $N$, the description of the initial-state population by $\text{tr}\rho_{\text{trunc}}(0)$ becomes less representative, leading to increasing systematic uncertainties, illustrated in Fig. 1(a). Here, the exponentially growing complexity becomes evident: $\dim(\mathcal{H}_{\text{trunc}}) \approx 2^{22}$ is required to achieve $\text{tr}\rho_{\text{trunc}}(0) = 0.99$ for $N = 5$. Figure 1(b) highlights the experimental controllability of $D_{\text{eff}}$. At $\{\Omega, \omega_z\} \approx \{2, 1\} \times \omega_1$, the strong coupling to numerous modes leads to a maximum in $D_{\text{eff}}$. For large $\omega_z$, the spin can get close to resonance with few modes only, the latter composing a comparatively small environment. Further, the range of accessible values of $D_{\text{eff}}$ grows with increasing $N$; see Fig. 1(c).

We experimentally implement the single spin by two electronic hyperfine ground states of $^{25}Mg^+$ and add up to four $^{26}Mg^+$ to engineer the size of the bosonic environment spanned by $N$ (number of ions) longitudinal (axial) motional modes. For details on our experimental setup, see Refs. [48,49]. First, we prepare the spin state, $\rho_S(0) = |\downarrow\rangle\langle\downarrow|$, by optical pumping and initialize the phonon state $\rho_E(0)$ by resolved sideband cooling [24] close to the ground state. In calibration measurements we determine that the modes are in thermal states with $\bar{n}_{j=1,\ldots,N} \lesssim 1$, which effectively enhances $\eta_{j=1,\ldots,N}$. Next,

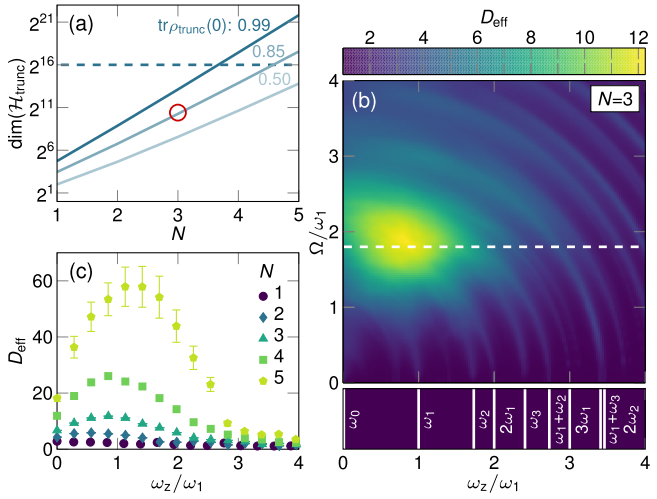


FIG. 1. Complexity of the Hamiltonian studied numerically. Parameters are $\omega_1/(2\pi) = 0.7$ MHz, $\bar{n}_{j=1,\ldots,N} = 1$. (a) Dimension of truncated Hilbert space $\dim[\mathcal{H}_{\text{trunc}}(N)]$ for corresponding fractions of initial-state population $\text{tr}\rho_{\text{trunc}}(0)$ lying within $\mathcal{H}_{\text{trunc}}$ (solid lines). For $N = 3$, for example, 85% lie within $\dim(\mathcal{H}_{\text{trunc}}) \approx 2^{10}$ (circle). We derive $D_{\text{eff}}(N, \Omega, \omega_z)$ up to $\dim(\mathcal{H}_{\text{trunc}}) = 2^{16}$ (dashed line). (b) Choosing $\Omega$ and varying $\omega_z$ (dashed line), we can tune the spin-phonon coupling into resonance with different modes (sketched at the bottom) and boost the system size. Note that the actual number of participating states is much larger than the normalized quantity $D_{\text{eff}}$; see Eq. (5). (c) For fixed $\Omega(N)$ [cf. dashed line in (b)], $D_{\text{eff}}(\omega_z)$ increases significantly with $N$. This enables the systematic investigation of equilibration and thermalization depending on the system size. Error bars show systematic numerical uncertainties [36].

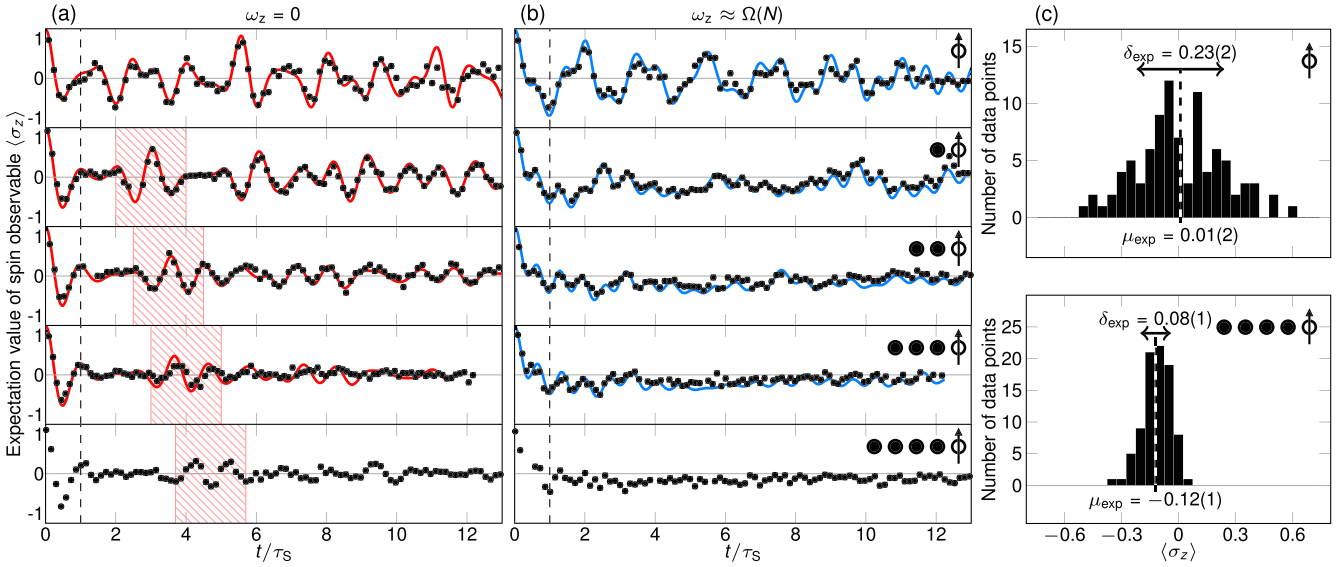


FIG. 2. Measured unitary time evolution $\langle\sigma_z(t)\rangle$. Experimental results (black dots, error bars: 1 s.d.) for $N = 1, \ldots, 5$ compared to full ED (solid lines). We exclude numerical results for $N = 5$ due to their large systematic uncertainties. Oscillations (time fluctuations) of high amplitude during the transient duration $t/\tau_S \lesssim 1$ are driven by the evolution of $\rho(0)$ towards the ground state of $H$. (a) For $\omega_z = 0$ and increasing $N$, excitation is coherently exchanged with a growing number of modes resulting in revivals at $\tau_{rev}$ (shaded areas). (b) For $\omega_z \approx \Omega(N)$, expectation values fluctuate around a negative offset. Revivals and this nontrivial bias emphasize the coherence of the dynamics. (c) Histograms of experimental measurements sample the probability distribution which underlies $\langle\sigma_z(t)\rangle$. Here, we show these for $t \in [\tau_S, 13\tau_S]$, $\omega_z \approx \Omega(N)$, and $N = 1, 5$ to exemplify the quantities $\mu_{exp}(\langle\sigma_z\rangle)$ and $\delta_{exp}(\langle\sigma_z\rangle)$.

we apply the spin-phonon interaction by continuously driving Raman transitions with spin coupling rate $\Omega$ for variable duration $t$, where $\omega_z$ is the controllable detuning from resonance [35]. Finally, we detect the spin by state-dependent fluorescence. We choose to record $\langle\sigma_z(t)\rangle$, while we numerically check that $\langle\sigma_{x,y}(t)\rangle$ feature similar behavior. To study dynamics for a large range of $D_{eff}$, we choose 95 parameter settings: We set $\omega_1/(2\pi) \approx 0.71$ MHz, which corresponds to an effective spin-phonon coupling parameter $\eta_{1,eff} \equiv \eta_1\sqrt{2\bar{n}_1 + 1} \approx 0.94$ for $\bar{n}_1 = 1$. For each $N = 1, \ldots, 5$, we use a fixed $\Omega(N)/(2\pi) = \{0.73(1), 0.95(3), 1.28(3), 1.37(3), 1.58(5)\}$ MHz and vary $\omega_z$ from 0 up to $4\omega_1$ [36].

In Fig. 2, we present two sets of $\langle\sigma_z(t)\rangle$ for $N = 1, \ldots, 5$. Each data point is obtained by averaging over $r = 500$ repetitions yielding an expectation value with statistical uncertainty $\propto 1/\sqrt{r}$. We compare $\langle\sigma_z(t)\rangle$ with numerical full ED of Eq. (1) with $\dim(\mathcal{H}_{trunc}) \leq 2^{13}$. As $N$ increases, the accuracy of numerical results decreases significantly. For $N = 4$, we have $\mathrm{tr}\rho_{trunc}(0) < 0.72$. For $N = 5$, since $\mathrm{tr}\rho_{trunc}(0) < 0.5$, we exclude numerical results in Figs. 2 and 3; here, even state-of-the-art full ED methods [16] could consider $\mathrm{tr}\rho_{trunc}(0) \lesssim 0.75$ only [36]. For $\omega_z = 0$ and $N = 1$, we confirm oscillations of high and persisting amplitude due to the coupling to the only mode at $\omega_1$. For increasing $N$, the spin couples to $N$ modes including higher order processes, such that spin excitation gets distributed (entangled) into the growing bosonic environment. Hence, coherent oscillations at incommensurate frequencies lose their common contrast and appear damped. After the transient duration $t/\tau_S \approx 1$, with $\tau_S \equiv 2\pi/\Omega$, the spin observable remains close to its time average. Still, the conservation of coherence of the evolution is evident in our measurements: Revivals of spin excitation due to the finite size of the system appear at $\tau_{rev} \sim 1/\overline{\delta E}$, where $\overline{\delta E}$ is the mean energy difference between modes. And, for $\omega_z \approx \Omega$, negative time averages of $\langle\sigma_z(t)\rangle$ indicate equilibration of the system to the ground state of $H$, biased by $\omega_z$. Both observations present strong independent evidence that our total spin-phonon system is near-perfectly isolated from external baths. Independent measurements yield a decoherence rate of $\gamma_{dec}\tau_S \approx 0.01$ [36]. This complements the agreement of experimental with numerical results, where we set $\gamma_{dec} = 0$.

We analyze all recorded time evolutions, each containing $S \approx 100$ data points in the interval $[\tau_S, 13\tau_S]$, by deriving time averages,

$$\mu_{exp}(\langle\sigma_z\rangle) \equiv \frac{1}{S}\sum_{t\in[\tau_S,13\tau_S]}\langle\sigma_z(t)\rangle, \tag{6}$$

and mean amplitudes of time fluctuations,

$$\delta_{exp}(\langle\sigma_z\rangle) \equiv \sqrt{\frac{1}{S-1}\sum_{t\in[\tau_S,13\tau_S]}[\langle\sigma_z(t)\rangle - \mu_{exp}(\langle\sigma_z\rangle)]^2}. \tag{7}$$

The quantities are illustrated in two examples in Fig. 2(c). We plot these in Fig. 3 for $N = 1, \ldots, 5$ and as a function of $\omega_z$, together with full ED results for $N = 1, \ldots, 4$ (solid lines). Tuning $\omega_z$ across the maximum of $D_{eff}$, cf. Fig. 1(b), and comparing $\mu_{exp}(\langle\sigma_z\rangle)$ to numerically calculated

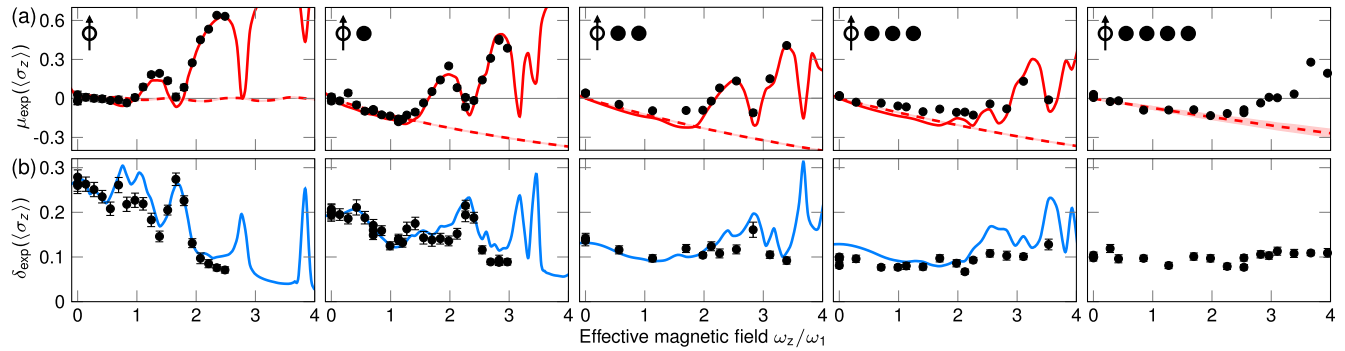


FIG. 3. Time averages and mean amplitudes of time fluctuations of $\langle\sigma_z(t)\rangle$. These are calculated from experimental traces (black dots, error bars: 1 s.d., derived from the underlying probability distribution of $\langle\sigma_z(t)\rangle$ [36]) for varying $\omega_z$ and $N = 1, \ldots, 5$ and comparison to full ED (solid lines). (a) Increasing $\omega_z$ shifts the ground state of $H$, adjusts spin-mode couplings, and varies $D_{\text{eff}}$. Even for small systems, we find agreement of time averages with microcanonical averages, $\mu_{\text{exp}}(\langle\sigma_z\rangle) \approx \mu_{\text{micro}}(\langle\sigma_z\rangle)$ (dashed lines, shaded areas indicate systematic uncertainties). As $D_{\text{eff}}$ rapidly increases with $N$, time averages follow microcanonical averages for a larger range of $\omega_z$. (b) $\delta_{\text{exp}}(\langle\sigma_z\rangle)$ gradually decreases with $N$, and correlated resonances in $\mu_{\text{exp}}(\langle\sigma_z\rangle)$ and $\delta_{\text{exp}}(\langle\sigma_z\rangle)$ fade away, indicating that we tune our system from microscopic to mesoscopic size.

microcanonical averages $\mu_{\text{micro}}(\langle\sigma_z\rangle)$ (dashed lines) [36], we find agreement for a larger range of $\omega_z$ when increasing $N$. This indicates an extended regime permitting thermalization. For large $\omega_z$, we observe its breakdown as the spin couples to an environment of decreasing complexity. Finite-size effects are prominent in resonances of $\mu_{\text{exp}}(\langle\sigma_z\rangle)$ and $\delta_{\text{exp}}(\langle\sigma_z\rangle)$ for $N = 1$, while their amplitudes gradually fade away for higher $N$.

For further analysis, we postselect data points well described by microcanonical averages, i.e., with a deviation of less than 0.1 [36]. For those, we show the dependence of $\delta_{\text{exp}}(\langle\sigma_z\rangle)$ on $N$ in Fig. 4(a). Although $N$ sets the size of the environment, the complexity of the spin-phonon coupling is tuned by $\Omega$, $\omega_z$, $\eta_1$, $\rho(0)$, and $N$, cf. Figs. 1(b) and 1(c). Consequently, we study the correlation between $\delta_{\text{exp}}(\langle\sigma_z\rangle)$ and $D_{\text{eff}}$ by combining our experimental results with numerical calculations of $D_{\text{eff}}$ in Fig. 4(b). In general, mean amplitudes of time fluctuations are predicted to be upper bounded by $1/\sqrt{d_{\text{eff}}}$. For our system, we even find a proportionality, $\delta_\infty(\langle\sigma_z\rangle) \propto 1/\sqrt{D_{\text{eff}}}$: We motivate this scaling, illustrated by the solid line in Fig. 4(b), by a heuristic derivation considering pure initial states and infinite times, which relies on the eigenstate thermalization hypothesis [36]. Our measurements feature such a scaling for $D_{\text{eff}} \lesssim 25$, despite our nonidealized initial states and finite observation duration. We observe that, for $D_{\text{eff}} \gtrsim 25$, measured mean amplitudes of time fluctuations do not further decrease. We attribute this to the fact that a system of increasing complexity features decreasing energy differences in its spectrum, corresponding to smaller relevant frequencies in the dynamics. Explicitly, the system requires longer durations to approach theoretically predicted values. Here, theory considers averages for infinite time, and does not make any prediction about relevant time scales in the dynamics.

In summary, we scale our trapped-ion system including its engineered environment up to relevant Hilbert space dimensions challenging state-of-the-art full ED. We present time averages and fluctuations of a spin observable and exploit an effective dimension to study their dependence on the size of the system. We observe the emergence of quantum statistical mechanics within our isolated system despite its moderate size. Simultaneously, we monitor the coherent dynamics of

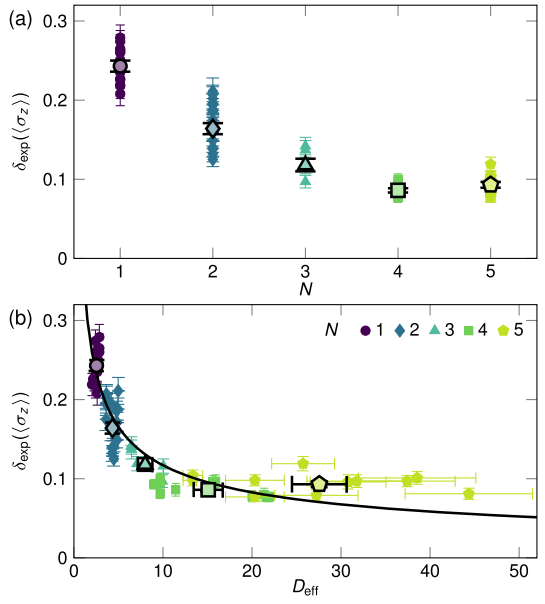


FIG. 4. Scaling of mean amplitudes of time fluctuations with $N$ and $D_{\text{eff}}$. (a) We plot $\delta_{\text{exp}}(\langle\sigma_z\rangle)$ (error bars: 1 s.d.) as a function of $N$. The spread for $N \leq 2$ highlights finite-size effects, and we show an average value for each $N$ (large symbols, error bars: 1 s.d.). For $N = 1, \ldots, 4$, we observe a decay that ceases for $N = 5$. (b) $\delta_{\text{exp}}(\langle\sigma_z\rangle)$ as a function of calculated $D_{\text{eff}}$ (error bars: systematic uncertainties), which captures the dependence of the effective system size on all experimental parameters. We compare to a scaling $\delta_\infty \propto 1/\sqrt{D_{\text{eff}}}$ (solid line), motivated for our system, and our measurements agree for $D_{\text{eff}} \lesssim 25$. Further increasing $D_{\text{eff}}$, the system needs longer durations to resolve decreasing energy differences in the environment, unveiling the importance of time scales.

thermalization, revealing the importance of initial and transient time scales by direct observation of the evolution towards thermal equilibrium. Thereby, we contribute to open questions in the field of thermalization [1,4,22]. Our approach admits generating a multitude of initial conditions, choosing different system and environment states, and preparing initial correlations [24,25,27]. In addition, it allows us to measure a variety of observables [24,27,50]. Applying those techniques, we can study, e.g., non-Markovianity of the dynamics, which is evidenced by revivals in the evolution, in detail [51,52]. Further, increasing the strength of the spin-phonon coupling, we can effectively expand the observable time span. Possible extensions include incorporating more and larger spins, tuning long-range interactions, adding external baths [30,35,53], and propelling experimental quantum simulations. Beyond numerical tractability, our experimental setup can be used as a test bed to assess the validity of approximated theoretical methods that address strong couplings to vibrational baths in a variety of fields, such as molecular and chemical physics.

We thank H.-P. Breuer for discussions, M. Enderlein, J. Pacer, and J. Harlos for assistance during the setup of the experiment, and M. Wittemer for comments on the manuscript. This work was supported by the Deutsche Forschungsgemeinschaft [SCHA 973; 91b (INST 39/828-1 and 39/901-1 FUGG)], the People Programme (Marie Curie Actions) of the European Union's Seventh Framework Programme (FP7/2007-2013, REA Grant Agreement No. PCIG14-GA-2013-630955) (D. P.), and the Freiburg Institute for Advanced Studies (FRIAS) (T. S.).

*Note added*—Recently, we became aware of related studies with trapped ions, superconducting qubits, and ultracold atoms [54–56].

*govinda.clos@physik.uni-freiburg.de

[1] S. Popescu, A. J. Short, and A. Winter, Nat. Phys. **2**, 754 (2006).
[2] S. Goldstein, J. L. Lebowitz, R. Tumulka, and N. Zanghì, Phys. Rev. Lett. **96**, 050403 (2006).
[3] P. Reimann, Phys. Rev. Lett. **101**, 190403 (2008).
[4] N. Linden, S. Popescu, A. J. Short, and A. Winter, Phys. Rev. E **79**, 061103 (2009).
[5] M. Cramer and J. Eisert, New J. Phys. **12**, 055020 (2010).
[6] A. J. Short and T. C. Farrelly, New J. Phys. **14**, 013063 (2012).
[7] A. Riera, C. Gogolin, and J. Eisert, Phys. Rev. Lett. **108**, 080402 (2012).
[8] J. M. Deutsch, Phys. Rev. A **43**, 2046 (1991).
[9] M. Srednicki, Phys. Rev. E **50**, 888 (1994).
[10] M. Srednicki, J. Phys. A **32**, 1163 (1999).
[11] M. Rigol, V. Dunjko, and M. Olshanii, Nature (London) **452**, 854 (2008).
[12] A. Polkovnikov, K. Sengupta, A. Silva, and M. Vengalattore, Rev. Mod. Phys. **83**, 863 (2011).
[13] L. D'Alessio, Y. Kafri, A. Polkovnikov, and M. Rigol, Adv. Phys. **65**, 239 (2016).
[14] M. Rigol, Phys. Rev. Lett. **103**, 100403 (2009).
[15] L. F. Santos and M. Rigol, Phys. Rev. E **81**, 036206 (2010).
[16] W. Beugeling, R. Moessner, and M. Haque, Phys. Rev. E **89**, 042112 (2014).
[17] H. Kim, T. N. Ikeda, and D. A. Huse, Phys. Rev. E **90**, 052105 (2014).
[18] M. Gring, M. Kuhnert, T. Langen, T. Kitagawa, B. Rauer, M. Schreitl, I. Mazets, D. A. Smith, E. Demler, and J. Schmiedmayer, Science **337**, 1318 (2012).
[19] S. Trotzky, Y.-A. Chen, A. Flesch, I. P. McCulloch, U. Schollwöck, J. Eisert, and I. Bloch, Nat. Phys. **8**, 325 (2012).
[20] T. Langen, S. Erne, R. Geiger, B. Rauer, T. Schweigler, M. Kuhnert, W. Rohringer, I. E. Mazets, T. Gasenzer, and J. Schmiedmayer, Science **348**, 207 (2015).
[21] M. A. Cazalilla and M. Rigol, New J. Phys. **12**, 055006 (2010).
[22] J. Eisert, M. Friesdorf, and C. Gogolin, Nat. Phys. **11**, 124 (2015).
[23] D. J. Wineland, C. Monroe, W. M. Itano, D. Leibfried, B. E. King, and D. M. Meekhof, J. Res. Natl. Inst. Stand. Technol. **103**, 259 (1998).
[24] D. Leibfried, R. Blatt, C. Monroe, and D. Wineland, Rev. Mod. Phys. **75**, 281 (2003).
[25] R. Blatt and D. Wineland, Nature (London) **453**, 1008 (2008).
[26] A. H. Myerson, D. J. Szwer, S. C. Webster, D. T. C. Allcock, M. J. Curtis, G. Imreh, J. A. Sherman, D. N. Stacey, A. M. Steane, and D. M. Lucas, Phys. Rev. Lett. **100**, 200502 (2008).
[27] D. Kienzler, H.-Y. Lo, B. Keitch, L. de Clercq, F. Leupold, F. Lindenfelser, M. Marinelli, V. Negnevitsky, and J. P. Home, Science **347**, 53 (2015).
[28] T. R. Tan, J. P. Gaebler, Y. Lin, Y. Wan, R. Bowler, D. Leibfried, and D. J. Wineland, Nature (London) **528**, 380 (2015).
[29] C. J. Ballance, V. M. Schäfer, J. P. Home, D. J. Szwer, S. C. Webster, D. T. C. Allcock, N. M. Linke, T. P. Harty, D. P. L. Aude Craik, D. N. Stacey, A. M. Steane, and D. M. Lucas, Nature (London) **528**, 384 (2015).
[30] D. Porras and J. I. Cirac, Phys. Rev. Lett. **92**, 207901 (2004).
[31] C. Schneider, D. Porras, and T. Schaetz, Rep. Prog. Phys. **75**, 024401 (2012).
[32] C. Monroe and J. Kim, Science **339**, 1164 (2013).
[33] M. Ramm, T. Pruttivarasin, and H. Häffner, New J. Phys. **16**, 063062 (2014).
[34] M. Mielenz, H. Kalis, M. Wittemer, F. Hakelberg, U. Warring, R. Schmied, M. Blain, P. Maunz, D. L. Moehring, D. Leibfried, and T. Schaetz, Nat. Commun. **7**, 11839 (2016).
[35] D. Porras, F. Marquardt, J. von Delft, and J. I. Cirac, Phys. Rev. A **78**, 010101 (2008).
[36] See Supplemental Material at http://link.aps.org/supplemental/10.1103/PhysRevLett.117.170401 for further details, which includes Refs. [37–46].
[37] D. Braak, Phys. Rev. Lett. **107**, 100401 (2011).
[38] J.-S. Caux and J. Mossel, J. Stat. Mech. (2011) P02023.
[39] U. Weiss, *Quantum Dissipative Systems* (World Scientific, Singapore, 1999).
[40] D. J. Luitz, N. Laflorencie, and F. Alet, Phys. Rev. B **91**, 081103 (2015).
[41] R. Mondaini, K. R. Fratus, M. Srednicki, and M. Rigol, Phys. Rev. E **93**, 032104 (2016).

[42] D. Hume Ph.D. thesis, University of Colorado at Boulder, 2010.
[43] A. Friedenauer, F. Markert, H. Schmitz, L. Petersen, S. Kahra, M. Herrmann, T. Udem, T. W. Haensch, and T. Schaetz, Appl. Phys. B **84**, 371 (2006).
[44] W. Ansbacher, Y. Li, and E. Pinnington, Phys. Lett. A **139**, 165 (1989).
[45] R. Ozeri, W. M. Itano, R. B. Blakestad, J. Britton, J. Chiaverini, J. D. Jost, C. Langer, D. Leibfried, R. Reichle, S. Seidelin, J. H. Wesenberg, and D. J. Wineland, Phys. Rev. A **75**, 042329 (2007).
[46] G. Casati, B. V. Chirikov, I. Guarneri, and F. M. Izrailev, Phys. Rev. E **48**, R1613 (1993).
[47] A. J. Leggett, S. Chakravarty, A. T. Dorsey, M. P. A. Fisher, A. Garg, and W. Zwerger, Rev. Mod. Phys. **59**, 1 (1987).
[48] T. Schaetz, A. Friedenauer, H. Schmitz, L. Petersen, and S. Kahra, J. Mod. Opt. **54**, 2317 (2007).
[49] G. Clos, M. Enderlein, U. Warring, T. Schaetz, and D. Leibfried, Phys. Rev. Lett. **112**, 113003 (2014).
[50] D. Leibfried, D. M. Meekhof, B. E. King, C. Monroe, W. M. Itano, and D. J. Wineland, Phys. Rev. Lett. **77**, 4281 (1996).
[51] H.-P. Breuer, E.-M. Laine, and J. Piilo, Phys. Rev. Lett. **103**, 210401 (2009).
[52] G. Clos and H.-P. Breuer, Phys. Rev. A **86**, 012115 (2012).
[53] C. J. Myatt, B. E. King, Q. A. Turchette, C. A. Sackett, D. Kielpinski, W. M. Itano, C. Monroe, and D. J. Wineland, Nature (London) **403**, 269 (2000).
[54] J. Smith, A. Lee, P. Richerme, B. Neyenhuis, P. W. Hess, P. Hauke, M. Heyl, D. A. Huse, and C. Monroe, Nat. Phys., doi: 10.1038/nphys3783 (2016).
[55] C. Neill *et al.*, Nat. Phys., doi: 10.1038/nphys3830 (2016).
[56] A. M. Kaufman, M. E. Tai, A. Lukin, M. Rispoli, R. Schittko, P. M. Preiss, and M. Greiner, Science **353**, 794 (2016).